Biophysical Journal Volume 101 December 2011 2807–2815

Analyzing the Homeostasis of Signaling Proteins by a Combination of Western Blot and Fluorescence Correlation Spectroscopy

Yi-Da Chung,[†] Michael D. Sinzinger,[†] Petra Bovee-Geurts,[†] Marina Krause,[†] Sip Dinkla,[†‡] Irma Joosten,[‡] Werner J. Koopman,[†] Merel J. W. Adjobo-Hermans,[†] and Roland Brock[†*]

[†]Department of Biochemistry, Nijmegen Centre for Molecular Life Sciences and [‡]Department of Laboratory Medicine, Laboratory of Medical Immunology, Radboud University Nijmegen Medical Centre, Nijmegen, The Netherlands

ABSTRACT The determination of intracellular protein concentrations is a prerequisite for understanding protein interaction networks in systems biology. Today, protein quantification is based either on mass spectrometry, which requires large cell numbers and sophisticated measurement protocols, or on quantitative Western blotting, which requires the expression and purification of a recombinant protein as a reference. Here, we present a method that uses a transiently expressed fluorescent fusion protein of the protein-of-interest as an easily accessible reference in small volumes of crude cell lysates. The concentration of the fusion protein is determined by fluorescence correlation spectroscopy, and this concentration is used to calibrate the intensity of bands on a Western blot. We applied this method to address cellular protein homeostasis by determining the concentrations of the plasma membrane-located transmembrane scaffolding protein LAT and soluble signaling proteins in naïve T cells and transformed T-cell lymphoma (Jurkat) cells (with the latter having nine times the volume of the former). Strikingly, the protein numbers of soluble proteins scaled with the cell volume, whereas that of the transmembrane protein LAT scaled with the membrane surface. This leads to significantly different stoichiometries of signaling proteins in transformed and naïve cells in concentration ranges that may translate directly into differences in complex formation.

INTRODUCTION

Over the past few decades, investigators have made enormous progress in identifying the constituents of cellular signaling networks and their functional interactions (1). The current challenge is to obtain quantitative parameters regarding concentrations, compartmentalization, and protein mobility to enable an understanding of the spatiotemporal dynamics in biological systems. Advanced microscopy techniques provide such information for compartmentalization and mobility (2). However, for the determination of protein concentrations, technological development has been lagging behind. Currently, the most common method is quantitative Western blotting (WB). In this method, a sample of the purified protein-of-interest of known concentration is used as an internal standard to determine the concentration of the respective protein in a complex mixture using antibody-based detection (3,4). However, the requirement to express and purify a recombinant protein is still a serious obstacle for the broad application of this technique. For example, transmembrane proteins are especially difficult to purify.

More recently, mass spectrometry-based techniques have been applied to both relative (5) and absolute (6) protein quantification. In these methods, internal standards can be generated by solid-phase peptide synthesis, which provides a significant advantage over the recombinant proteins required for WB-based methods. In addition, no antibodies or other affinity-based binders are required for detection. Disadvantages of the mass spectrometry-based methods include the need for sophisticated equipment and data analysis infrastructure, and high numbers of cells (in the range of hundreds of millions).

In this study, we aimed to overcome the limitations of the current techniques by providing a method that obviates the need to purify a protein standard and requires only a relatively small number of cells. The latter is especially important for cells that are difficult to expand ex vivo, such as naïve T cells. A transiently expressed fluorescent protein (FP) fusion protein of the protein-of-interest serves as an internal standard. The concentration of the FP is determined in crude cell lysates by fluorescence correlation spectroscopy (FCS) (7,8). FCS provides direct quantitative information about molecular mobility and the number of fluorescent particles that are present in the confocal detection volume. This information is extracted from fluctuations of fluorescence caused by diffusion of molecules through the femtoliter-size confocal detection volume (9–11). With knowledge about the size of the confocal detection volume, one can convert these figures into concentrations. FCS works best at molecule concentrations in the lower nanomolar range.

We applied our FCS-based protocol to determine the concentrations of proteins involved in early T-cell receptor signaling, a cellular signaling cascade that plays a central role in the orchestration of a cellular immune response. Upon receptor activation, the transmembrane scaffolding protein Linker for Activation of T cells (LAT) (12) is phosphorylated at multiple tyrosines, which constitute binding sites for proteins containing SH2 domains (13), including the adaptor proteins GRB2 and GADS (14) and the

Submitted April 28, 2011, and accepted for publication September 26, 2011.

*Correspondence: R.Brock@ncmls.ru.nl

Editor: Petra Schwille.

0006-3495/11/12/2807/9 $2.00

doi: 10.1016/j.bpj.2011.09.058

phosphotyrosine phosphatase SHP1 (15). For SH2 domains, binding preferences overlap (16,17). Therefore, inside a cell, proteins compete for binding sites (17). As a consequence, the nature of the formed molecular complexes is a function not only of the identity of the present proteins and the relative dissociation constants of the individual pairs of interactions, but also of their concentrations. Moreover, by comparing Jurkat T-cell leukemia cells and human $CD4^+$ T cells, which differ considerably in size, we sought to determine the degree to which molecule numbers scale with size, i.e., whether concentrations are cell-size invariant.

MATERIALS AND METHODS

Transfection of FP fusions

Jurkat T cells were maintained in RPMI 1640 medium (PAN Biotech, Aidenbach, Germany) supplemented with 10% (v/v) heat-inactivated fetal bovine serum (PAN Biotech) and passaged every 2–3 days. Cells for transfection were cultured until log phase (2 days) and spun down at 340 × *g* for 5 min. Then, the cells were resuspended in RPMI 1640 without phenol red (PAN Biotech) at a cell density of 5×10^7 cells/ml. Plasmid DNA (5 μg) was added to a 100 μl cell suspension in a 2-mm electroporation cuvette with a short electrode (PEQ LAB Biotechnologie, Erlangen, Germany). The cell suspension was electroporated with plasmids encoding for the respective fusion proteins (see Section S1 of the Supporting Material) at 180 V, 900 μF, and 200 Ω (Gene Pulser; Bio-Rad, Veenendaal, The Netherlands). The electroporated cells were transferred into six-well plates (Greiner Bio-One, Alphen aan den Rijn, The Netherlands) containing 5 ml RPMI 1640 medium, supplemented with 5% fetal bovine serum, and cultured for 24 h at 37°C in 5% CO_2.

Isolation of $CD4^+$ T cells

We obtained buffy coats (Sanquin Bloodbank, Nijmegen, The Netherlands) from healthy human donors after they provided written informed consent with regard to scientific use. Peripheral blood mononuclear cells were isolated by density gradient centrifugation (Lymphoprep; Nycomed Pharma, Roskilde, Denmark). We then isolated $CD4^+$ T cells enriched by MACS sorting, using 15 μl anti-CD4 magnetic microbeads per 10^7 cells, according to the manufacturer's instructions (Miltenyi Biotec, Bergisch Gladbach, Germany).

Preparation of cell lysates

Cells were harvested by centrifugation at room temperature for 5 min at 340 × *g*. The pellet was washed once in HBS buffer (10 mM Hepes, 135 mM NaCl, 5 mM KCl, 1 mM $MgCl_2$, 1.8 mM $CaCl_2$, and pH 7.4) and the proteins were extracted by adding lysis buffer (20 mM Tris, 1% Triton X-100, 1 mM EDTA, 150 mM NaCl, 1 mM Na_3VO_4, 1× complete protease inhibitor cocktail (Roche, Mannheim, Germany), 50 mM octyl-β-D-glucopyranoside (Fluka, Zwijndrecht, The Netherlands), pH 7.5) at a concentration of 2×10^7 cells/ml. Lysates were kept on ice for 1 h. After centrifugation (15 min, 20,000 × *g*, 4°C), the supernatant was used for FCS analyses and WB.

FCS measurements

FCS measurements were performed on a Leica TCS SP5 laser scanning confocal microscope equipped with a dual-channel FCS module (Leica Microsystems, Rijswijk, The Netherlands) and a Plan APO 63 × 1.2 NA water-immersion lens. The emitted fluorescence was split by a BS 560 beam-splitter and passed a BP 500–550 band-pass filter for channel 1 (mEGFP) and BP 607-683 for channel 2 (mCherry) detection. For real-time correlation of raw data, we used Vista FCS software (ISS, Champaign, IL). All measurements were performed at 37°C. We calibrated the instrument using standards of 20 nM fluorescein in 10 mM Tris/HCl buffer (pH 8.0) for channel 1 (green) and 20 nM Texas Red (Sulforhodamine 101 chloride; Sigma, Zwijndrecht, The Netherlands) in PBS buffer (pH 7.4) for channel 2 (red). The samples were loaded into a 348-well plate (Molecular Machines and Industries, Glattburg, Switzerland) with a thin glass bottom that suits FCS measurements. Before measurements were conducted, the wells were coated with PBS containing 0.1% BSA for 15 min. We obtained FCS measurements in five repeats of 50 s for each sample, using 15.6 μW of the 488 nm line of an Argon-ion laser for fluorescein and EGFP, and 9.9 μW of a 594 nm HeNe laser for Texas Red and mCherry excitation, as measured at the exit aperture of the lens using an X1-1 laser power meter (Gigahertz-Optik, Puchheim, Germany) equipped with an LSM-9901 Luminous Flux detector head. Cell lysates were measured under the same conditions as the fluorophore standards.

The autocorrelation functions $G(\tau)$ of five repeats for each sample were globally fitted with the use of a 3D Gaussian triplet model. This model accounts for one diffusing component and one photophysical transition, such as a triplet state, as shown in Eq. 1:

$$G(\tau) = \left(1 + \left(\frac{T}{1-T}\right) \cdot e^{-(\tau/\tau_T)}\right) \cdot \frac{1}{N} \cdot \frac{1}{1 + (\tau/\tau_D)} \cdot \frac{1}{(1 + (S^{-2} \cdot (\tau/\tau_D)))^{1/2}} \quad (1)$$

where T and τ_T respectively represent the fraction and the relaxation time of a photophysical transition between a fluorescence emitting and a dark state, which corresponds to so-called blinking in the case of FPs (18,19). N represents the average particle number in the confocal detection volume, and τ_D is the characteristic dwell time of the fluorophores in the confocal detection volume. The structure parameter S describes the ratio of axial to radial radii of the detection volume. Autocorrelation functions of repeated measurements were globally fitted by linking all variable parameters. The structure parameter S and τ_T were kept fixed. S was determined by calibration measurements of standard fluorophores, and τ_T was determined by acquiring autocorrelation functions with increasing pinhole diameters to separate the diffusional contribution to the autocorrelation function from the blinking time constant of the FPs (Section S2). For each set of experiments, background fluorescence was acquired from cell lysates of nontransfected Jurkat T cells. The background-corrected number of particles (N_{corr}) of fluorescent fusion proteins was calculated according to Eq. 2, with N_{raw} corresponding to the particle number derived from Eq. 1, I_{total} the total fluorescence, and I_b the background signal of the lysate:

$$N_{corr} = N_{raw} \cdot \left(1 - \frac{I_b}{I_{total}}\right)^2 \quad (2)$$

This correction eliminates an overestimation of molecule numbers caused by a decrease of the autocorrelation amplitude through uncorrelated background (20). The effective detection volume was determined by direct measurement of point-spread functions (PSFs; Section S3). We then calculated the concentration of the FP by dividing N_{corr} through the effective confocal detection volume.

Western blot

For the analysis of serial dilutions by SDS-PAGE, the sample order was randomized to eliminate trends in the densitometric analysis caused by an inhomogeneous background (4). After performing SDS-PAGE, for

WB we transferred the proteins from the gels onto PVDF membranes using an iBlot Gel Transfer Device (Invitrogen, Breda, The Netherlands). Blocking of membranes, incubation with antibodies, washing, and scanning were carried out on an Odyssey infrared imaging system (Li-Cor Biosciences, Lincoln, NE) according to the manufacturer's specifications, using antibodies as described in Section S4. Fluorescence was visualized and quantified via the Odyssey infrared imaging system. Rectangular regions of interest (ROIs) were selected manually to cover the entire target band. Neighboring ROIs of the same size were selected to determine the background intensity.

Determining fractions of fluorescing fusion proteins

We determined the concentrations of purified EGFP and mCherry proteins (kind gifts from V. Subramaniam, University of Twente, and J. Goedhart, University of Amsterdam) by running various amounts of these proteins next to a BSA standard on a 12% SDS-polyacrylamide gel. After electrophoresis, the proteins were stained with Coomassie Blue (Bio-Safe Coomassie, Bio-Rad). We visualized the gels using the 700 nm emission channel of the Odyssey infrared imaging system, and quantified purified FPs by comparison with the BSA standard, assuming equal emissions per gram of protein.

Next, we analyzed different amounts of the purified FPs next to several dilutions of lysates of cells expressing fusion FPs by WB as described in the previous section. Purified FPs with known total protein concentration served as standards for determining total FP concentration of lysates. FCS measurements were performed under identical conditions for lysates of cells expressing the fusion FPs and for the purified FPs. Background-corrected particle numbers were used to calculate fluorescing protein concentrations. We then calculated the fraction of fluorescing FP by relating the concentration of fluorescent molecules determined by FCS to the total concentration determined by WB.

RESULTS AND DISCUSSIONS

The cloning and transient expression of a fluorescent fusion protein in mammalian cells are more straightforward than the expression and purification of the recombinant protein. Because FCS offers the unique possibility of directly determining concentrations of fluorescent particles, we decided to explore the use of FCS as a means to calibrate intensities of protein bands in WB (Fig. 1). The FCS-based calibration of concentrations thus replaces calibration based on known amounts of purified recombinant proteins. In our case, we made use of the enhanced form of the green FP (EGFP) and the monomeric variant of the red-FP mCherry (21). We selected these two FP variants to explore factors that affect the suitability of the FCS-based approach and to enable further applications of the fusion proteins, in which the interaction of signaling proteins is addressed by dual-channel fluorescence techniques such as fluorescence cross-correlation spectroscopy (22,23).

Fractions of fluorescing fusion proteins

A critical parameter for calibration protocols based on FPs is the fraction of proteins that really show fluorescence. An inability to fluoresce may be due to compromised chromophore formation or function (24,25). If fluorescence is not shown by a fraction of FPs, FCS-based detection will underestimate the protein concentration. Therefore, we first determined the fractions of fluorescing proteins for various fusion proteins using purified recombinant mCherry and EGFP as standards (Fig. 2 *A*).

Given the relevance of protein concentrations for understanding the organization of protein complexes in T lymphocytes, we selected Jurkat T-cell leukemia cells as a cell line. The cells were transiently transfected with plasmids encoding proteins involved in T-cell signaling, i.e., the SH2 domain-containing proteins GRB2, GADS, and SHP1 fused to mCherry, and the scaffolding transmembrane

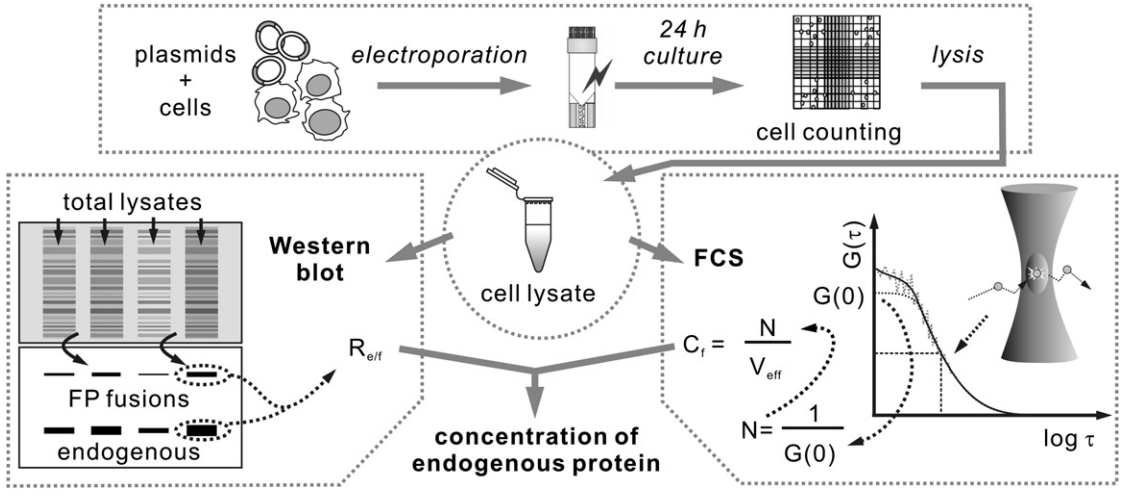

FIGURE 1 Determination of cellular protein concentrations using FCS for calibration of WB. Lysates of cells transiently expressing the protein of interest fused to an FP are analyzed in parallel by FCS and WB. With knowledge of the confocal detection volume V_{eff} (Section S3), the molecule number *N* obtained by FCS is converted into a concentration of FP (C_f) in the lysate. This concentration is then used to calculate the endogenous protein concentration through determination of the ratio ($R_{e/f}$) between the endogenous and recombinant fluorescent fusion protein, as obtained from WB analysis.

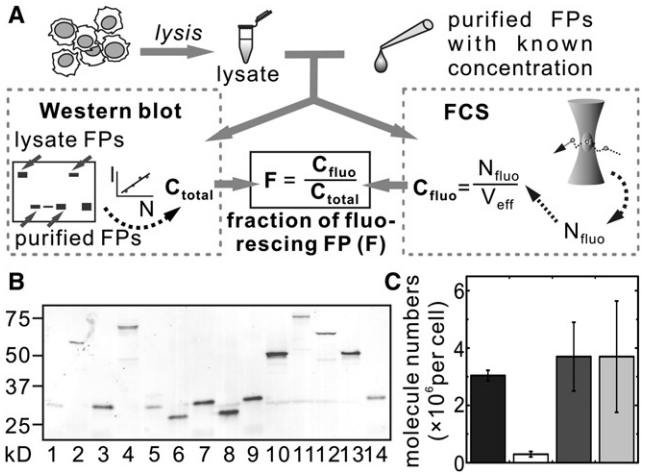

FIGURE 2 Determination of the fraction of fluorescing fusion proteins. (*A*) Scheme depicting the protocol for determining the fraction of fluorescing fusion proteins. Concentrations of FPs (C_{fluo}) are derived from the number of fluorescent molecules (N_{fluo}), as provided by FCS, divided by the confocal detection volume (V_{eff}). The concentration of total FP (C_{total}) is determined by using standard quantitative WB of known amounts of purified FPs as a standard and probing with an antibody against FP. Band intensities (I) for purified FPs on WB versus the respective molecule numbers (*N*) in the samples are plotted as a standard curve for determining unknown samples. The fluorescent fraction of FP (F) is given by the ratio C_{fluo}/C_{total}. (*B*) WB of FPs probed with an antibody against monomeric DsRed for detection of mCherry. Different amounts of cell lysates or recombinant proteins were loaded into the individual lanes (lanes 1, 3, 5, 7, 9, and 14: purified mCherry; lanes 2 and 12: mCh-GADS; lanes 4 and 11: mCh-SHP1; lanes 6 and 8: transiently expressed mCherry; lanes 10 and 13: mCh-GRB2). (*C*) Comparison of the endogenous GRB2 concentration determined by the conventional quantitative WB method (*black bar*) and the FCS-based method without (*white bar*) and with (*gray bars*) correction of the fraction of fluorescing proteins, without (*left*) and with (*right*) propagation of the error for fluorescing fractions of FPs.

protein LAT fused to EGFP. Moreover, we transfected plasmids encoding free mCherry and EGFP.

First, we determined the concentrations of the purified recombinant FPs by SDS-PAGE and Coomassie Brilliant Blue staining using BSA as a standard. Next, different amounts of purified FPs and fluorescent fusion protein-containing cell lysates were analyzed by WB and probed with antibodies against the FP part of the fusion protein (Fig. 2 *B*). FCS measurements were conducted on aliquots of the same samples, and finally, the number of fluorescent particles in the lysates was related to the intensities of the lanes in the WB. Considerable differences were found for the individual proteins (Table 1). Interestingly, the highest relative fractions of fluorescent particles were detected for the transiently expressed free EGFP and mCherry. Therefore, we used the fractions for transiently expressed free EGFP and mCherry to normalize the fractions of FPs for other FP samples. With this normalization for the mCherry fusion proteins, the fractions of FPs varied between 8% and 36% of the maximum. Likewise, the fluorescent fractions of the purified EGFP and mCherry were determined as 44% and 36%, respectively (Table 1). To validate the FCS-based approach and obtain an absolute determination of fluorescing fractions, we determined the fractions of fluorescing purified FPs by UV/Vis spectroscopy (Section S5, Fig. S3). This approach yielded fractions of fluorescent particles of 53% for purified EGFP and 47% for purified mCherry, in agreement with the values determined by FCS. The transiently expressed FPs in crude cell lysates therefore constitute a valid standard that reflects fully fluorescing FP, obviating the need to use purified FPs.

TABLE 1 Fractions of fluorescing fusion proteins

Fluorescent fusions	Fraction of fluorescing proteins
Free mCherry	1.00
Purified mCherry	0.36 ± 0.21
mCh-GRB2	0.08 ± 0.03
mCh-GADS	0.12 ± 0.04
mCh-SHP1	0.34 ± 0.13
Free EGFP	1.00
Purified EGFP	0.44 ± 0.33
LAT-EGFP	0.37 ± 0.22

Transient expression of nonconjugated FPs in Jurkat cells gave the highest number of fluorescing proteins and was therefore assumed as one and used for normalization. Values are shown as the mean ± SD from at least three independent experiments relative to free mCherry and free EGFP.

Our results revealed considerable differences in the fraction of fluorescing proteins. The fraction of fluorescing FP fusion proteins is an important parameter to consider when using FPs for quantitative microscopy (24,25). Several parameters influence the fraction of fluorescing proteins. The chromophore may not be formed or it may not be in a properly arranged protein environment. Furthermore, fluorophores may show blinking between fluorescence-active and -inactive states (26). Ample evidence indicates that the degree and kinetics of chromophore formation vary between individual fusion proteins (21,25,27). The higher fraction of fluorescing proteins expressed in mammalian cells is in line with previous observations that chaperones assist the folding and chromophore formation of FPs (28,29). Also, it was observed that fusion of FPs may particularly interfere with the folding of multidomain proteins (28). The molecular basis for the extreme behavior of the mCherry-GRB2 fusion remains elusive. Sequencing revealed no mutations. Slower folding and/or rapid turnover of the protein may decrease the steady-state levels of FPs with a readily formed chromophore. The different reactivities of the antibody used for detection toward the free and fusion proteins do not provide an explanation. If the anti-FP antibody is more reactive to the free FP than to the fusion protein, the fraction of FPs would be over- rather than underestimated. Because the fraction of fluorescent FP is affected by the kinetics of protein turnover, it will be interesting to further explore the extent to which this combination of FCS and WB might complement the growing repertoire of FP-based methods for determining protein stabilities (30,31).

Determining concentration by a combination of FCS and WB

We first sought to determine the protein concentrations by using an mCherry fusion protein of GRB2, which we also purified as a recombinant protein to compare the results obtained with the FCS-based method with those obtained by standard WB (Section S6). Jurkat cells were transiently transfected with mCherry-GRB2. Cell lysates were prepared and aliquots were used in parallel for both quantitative WB analyses (Fig. 3 *A*) and FCS measurements. We determined the ratio between fluorescent fusion protein and endogenous protein by plotting background-corrected band intensities derived from lysates of different cell numbers (Fig. 3 *B*). These plots confirmed the linearity of the blot scanner over the selected concentration ranges. We loaded the samples in a randomized order to eliminate drifts in the gel that might otherwise compromise the quantitative analyses of band intensities (4). FCS measurements provided fluorescent molecule numbers corresponding to particular band intensities (Fig. 3 *C*). The molecule numbers in the confocal detection volume were converted into molecular concentrations in the lysate and corrected for the fraction of fluorescent molecules. We derived the FCS detection volumes from experimentally measured PSFs using subresolution fluorescent beads (Section S3). This method does not require a priori knowledge about the diffusion constants, as is required when the dimensions of the detection volume are recovered from the decay behavior of the autocorrelation function, and is robust toward errors in the dilution of fluorescent dyes, as is the case when calibration occurs via known concentrations of fluorophores (32). Cross-validation of the PSF-based approach using a published diffusion constant yielded an excellent agreement (33) (Table S1). We then calculated the endogenous protein concentration in the lysate by simply combining the concentration of the fluorescent fusion protein (as determined by FCS) and the ratio between fluorescent recombinant and endogenous proteins (as determined by WB). This protocol yielded an intracellular molecule number of $3.70 \pm 1.20 \times 10^6$ for GRB2 in Jurkat cells (Fig. 2 *C* and Table 2). The standard quantitative WB yielded a result of $3.04 \pm 0.18 \times 10^6$ molecules per cell, demonstrating a good agreement between the two methods (Fig. 2 *C*). We also applied the FCS-based approach to determine the endogenous protein concentrations of GADS, SHP1, and LAT. For the two SH2 domain-containing proteins, GADS and SHP1, the molecule numbers per cell were comparable to those found for GRB2, i.e., 4.45×10^6 and 3.4×10^6, respectively. In contrast, for LAT, only 0.37×10^6 copies were found to be present per cell (Table 2).

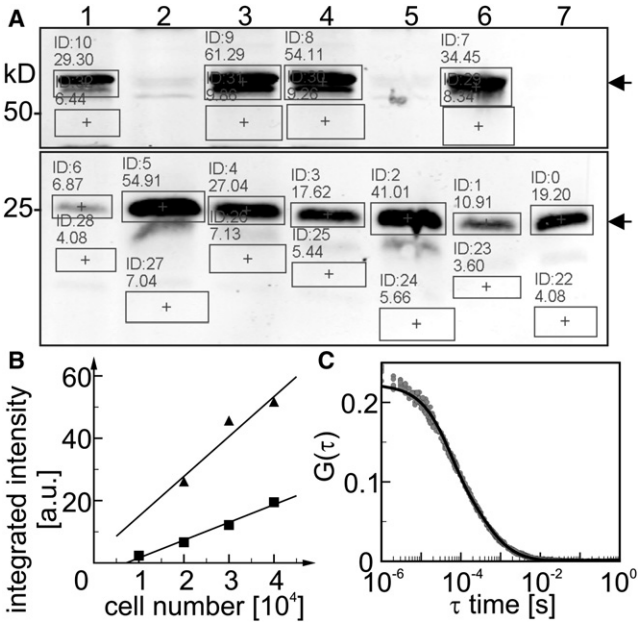

FIGURE 3 Determination of endogenous GRB2. (*A*) WB of lysates of mCherry and mCherry-GRB2-transfected Jurkat cells probed with an anti-GRB2 antibody. Samples containing different amounts of lysate were loaded in a randomized fashion to compensate for drift in the gel. Lanes 2, 5, and 7 contain various volumes of lysates of mCherry-transfected cells. Lanes 1, 3, 4, and 6 contain various volumes of lysates of mCh-GRB2-transfected cells. The arrowhead in the upper panel indicates mCh-GRB2, and the one in the lower panel indicates the endogenous GRB2. (*B*) Linear regression analysis of background-corrected intensities of endogenous GRB2 (*solid squares*) and mCh-GRB2 (*solid triangles*) plotted versus cell numbers. (*C*) Autocorrelation functions of mCh-GRB2 in crude cell lysates. The global fit to the autocorrelation function is indicated as a solid black curve. Average numbers of molecules were derived from the amplitude of fitted autocorrelation curves.

The reliability of the FCS-based method was high. All experiments yielded sufficiently high expression levels of fusion proteins in the lysate and WB. Nevertheless, even though the same protocol was used for transfection each time, the concentrations of fusion proteins in the lysate varied by up to one order of magnitude. This may be attributed to the fact that Jurkat cells are a difficult-to-transfect cell line, and transfection yields vary with the passage number. The transient expression of the FP had no effect on endogenous protein levels. This may be due to the rather short cultivation time before lysis (Section S7 and Fig. S4). For GRB2 and SHP1, one measurement each out of nine and eight, respectively, yielded an endogenous protein number that was higher than the mean by >1.5 times the standard deviation (SD).

The relative error was larger for the FCS-based approach than for the quantitative WB. For GRB2, the CV for the standard WB-based quantification method was 6%, in comparison with 30% for the FCS-based method. A source of uncertainty was the determination of the fluorescing fraction of the individual fusion proteins. When the error propagation was included, the CV increased to 52% (Fig. 2 *C*). Here, we determined the average fluorescing fractions in independent experiments assuming that this was a constant. In the future, it will be interesting to determine the fluorescing fractions in parallel with the protein concentrations

TABLE 2 Cellular molecule numbers and concentrations of endogenous proteins

	Jurkat			CD4$^+$ T cell		
		Concentration (μM) or surface density* (No./μm^2)			Concentration (μM) or surface density* (No./μm^2)	
Proteins	Cellular molecule number ($\times$ 10^6/cell)	Whole cell	Nucleus excluded	Cellular molecule number ($\times$ 10^6/cell)	Whole cell	Nucleus excluded
GRB2	3.70 ± 1.20/1.94 (n = 8/9)[†]	3.02 ± 0.98/1.59	4.90 ± 1.59/2.57	0.34 ± 0.10 (n = 4)[‡]	2.49 ± 0.71	10.42 ± 2.98
GADS	4.45 ± 2.15/2.58 (n = 7/7)	3.63 ± 1.76/2.11	5.89 ± 2.85/3.42	n/d	n/d	n/d
SHP1	3.40 ± 0.99/1.67 (n = 7/8)[†]	2.78 ± 0.81/1.37	4.50 ± 1.31/2.21	0.25 ± 0.09/0.13 (n = 3)	1.82 ± 0.66/0.98	7.61 ± 2.77/4.09
LAT	0.37 ± 0.18/0.29 (n = 7/7)	0.30 ± 0.15/0.24 472 ± 236/373*	0.48 ± 0.24/0.38 n/a	0.15 ± 0.03/0.10 (n = 4)	1.11 ± 0.25/0.73 843 ± 192/551*	4.65 ± 1.06/3.04 n/a

Total cellular and nuclear volumes were determined by confocal laser scanning microscopy (Section S9). Numbers of independent experiments (n) are given and values are shown as the mean ± SD without error propagation/SD with error propagation (fluorescing fraction of FP).
n/d, not determined; n/a, not applicable.
*For LAT, the surface density is also given in unit of molecules per μm^2.
[†]Outliers $\gtrless 1.5 \times$ SD were omitted from the calculation of the mean. Shown are the total number of measurements and the number of measurements that were within the 1.5 SD limits.
[‡]This result combines one result obtained by the novel method with three obtained by standard quantitative WB; thus, no SD with error propagation was available.

for the same samples, and to increase the number of experiments for determining fluorescing fractions. Nevertheless, the accuracy of the FCS-based method was high. For GRB2, the concentrations determined with both the conventional and new approaches differed by only 20%.

With respect to concentration range, because protein concentrations can always be adjusted by dilution, there is no upper concentration limit. This is especially the case if the fluorescent fusion protein is expressed in a different cell line and this cell lysate can be diluted independently from the lysate for which the concentration of endogenous protein is to be determined. Concerning the lower end of the concentration range, the availability of high-affinity antibodies will be decisive. We do not consider the sensitivity of FCS a limiting factor. For all of the transfected proteins, we achieved expression levels that were compatible with FCS, which has a subnanomolar sensitivity.

An analysis of the counts per molecule (cpm), which is a measure for protein aggregate formation as well as for the presence of uncorrelated background (34), demonstrated that neither of these factors was a concern. Within an error range of 10–30%, the cpm for all fusion proteins was identical to that of the free fusion proteins (data not shown).

Subcellular localization of T-cell signaling proteins

For the control of molecular interactions, the local concentrations in the relevant subcellular compartments are decisive. For all of the proteins, both the fusion protein and the endogenous protein displayed a similar subcellular localization, demonstrating that fusion to the FP does not change protein distribution (Fig. 4). GRB2, GADS, and SHP1 were all homogeneously distributed within the cytoplasm of Jurkat T cells (Fig. 4), and GRB2 and (to some degree) GADS were also detected in the nucleus. LAT was located in the plasma membrane, except for a structure resembling the microtubule-organizing center, in agreement with previous findings (35). A somewhat higher granularity of the immunofluorescence staining in comparison with the fusion proteins was a characteristic of the staining protocol, as cross-validated by immunofluorescence of fusion-protein-expressing cells (Section S8 and Fig. S5).

Concentrations of signaling proteins in CD4$^+$ T cells versus Jurkat cells

In addition to Jurkat cells, we were interested in extending the FCS-based quantification to naïve human CD4$^+$ T cells, the nontransformed counterpart of Jurkat T-cell leukemia cells. Jurkat and naïve human CD4$^+$ T cells differ considerably in size. Because molecular interactions are governed by the concentrations of interacting molecules,

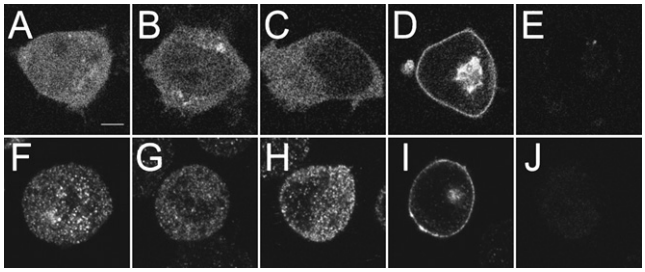

FIGURE 4 Intracellular protein distribution. GRB2 (*A* and *F*), GADS (*B* and *G*), SHP1 (*C* and *H*), and LAT (*D* and *I*) were either expressed as fluorescent fusion proteins (*A–D*) or detected by immunofluorescence (*F–I*). (*E* and *J*) Autofluorescence controls were either not transfected (*E*) or incubated only with secondary antibody (*J*). Scale bar indicates 5 μm.

for freely diffusive proteins such as GRB2, one should therefore postulate that molecule numbers scale with cell size.

Because naïve T lymphocytes are difficult to transfect, we loaded lysates of transiently transfected Jurkat cells next to lysates of naïve T cells. Band intensities were referenced between lanes. This analysis was conducted for GRB2, SHP1, and LAT in $CD4^+$ T cells (Table 2). For GRB2 and SHP1, the molecule numbers in $CD4^+$ T cells were only 9% and 7%, respectively, of those determined for the Jurkat cells, compared with 41% for the transmembrane protein LAT (Table 2).

To convert these molecule numbers into concentrations for both the whole cells and the cytoplasm only, we determined the volumes of whole cells and nuclei using confocal microscopy (Section S9). Using these volumes, we converted the molecule numbers for GRB2, GADS, and SHP1 into cellular concentrations for the whole cell and the cytoplasm only (Table 2). For LAT, in addition to the concentrations, we calculated the surface densities by assuming a sphere-like cell shape. In Jurkat cells, the concentrations of the cytoplasmic proteins (GRB2, GADS, and SHP1) were ~3 μM. Exclusion of the nuclear volume had only a small effect on the protein concentrations.

In naïve $CD4^+$ T cells, the molecule numbers corresponded to intracellular concentrations of ~1–2.5 μM when related to the whole cell volume. However, the nucleus of $CD4^+$ T cells comprises a larger fraction of the total cell volume as compared with Jurkat cells (Table S2). Therefore, relating the molecule numbers to the cytoplasm only had a stronger effect on protein concentrations in $CD4^+$ T cells. For SHP1, the concentration in $CD4^+$ T cells was about twice as high as that in Jurkat cells. Overall, the protein concentrations, but not the molecule numbers of the soluble proteins, were largely invariant to cell volume.

Only a few studies have reported on the concentration of proteins in cells, mainly due to the lack of robust and convenient methods for measuring protein concentrations. Therefore, in modeling studies on complex formation and signaling networks, investigators often make assumptions for cellular protein concentrations (36). Hanke et al. (37) reported GRB2 concentrations of ~0.5 μM as determined by stable isotope labeling by amino acids in cell culture (SILAC) in HeLa, HepG2, and C2C12 cells; however, to our knowledge, no data on GRB2 concentrations in T cells have been published. For SHP1, other authors reported a comparable concentration or one that exceeds our concentrations by up to one order of magnitude (38–40).

For the transmembrane protein LAT, relating the molecule numbers to cell volume yielded concentrations of 0.3 μM in Jurkat cells and 1.1 μM in naïve $CD4^+$ T cells, which differed by a factor of 3.7 (Table 2). However, for a transmembrane protein, surface density should be decisive with respect to the organization of protein complexes. When we related the molecule number per cell to the surface area, the surface densities between Jurkat and $CD4^+$ T cells differed by only a factor of 2 (Table 2). This higher surface density of LAT in $CD4^+$ T cells was cross-validated by anti-LAT immunofluorescence and detection of membrane-associated fluorescence by confocal detection (Section S10). These data show that the number of transmembrane LAT proteins scales with surface area, whereas the number of cytosolic proteins (i.e., GRB2 and SHP1) scales with cell volume. These results suggest that the expression of transmembrane proteins and soluble signaling proteins is subject to regulatory processes that sense surface density and intracellular concentration. Further analyses in relevant pairs of naïve cells and counterparts of larger size, such as naïve and activated B- and T-lymphocytes, and cells in different stages of the cell cycle, will reveal the general relevance of this observation. Importantly, however, even though concentrations and densities correlate with volume and surface area, respectively, the differences in cell size nevertheless lead to a different ratio between LAT and its binding partners, which may ultimately affect the formation of complexes. Taking GRB2 as an example, in Jurkat cells this ratio was 11:1 whereas in naïve $CD4^+$ T cells it was 2:1. Previous studies suggested that several GRB2 proteins bind one LAT molecule to sustain TCR-mediated signaling (36,41,42). Thus, at the low stoichiometries of GRB2 over LAT in naïve T cells, the number of GRB2 molecules may become limiting (Section 11 and Table S3).

CONCLUSIONS

In summary, we implemented FCS as a powerful calibration method to extract absolute molecule numbers from WBs. In comparison with established protocols, this approach circumvents the purification of recombinant proteins, which can be a major difficulty in protein quantification. Especially for transmembrane proteins, this characteristic is an asset. cDNAs for the expression of fusion proteins can be generated and transiently transfected by routine procedures. Importantly, only a few million cells are required for one set of experiments including both FCS measurements and WB analysis. Because it uses easily transfectable cells as a source of the fusion protein, the method is also applicable to cells that are more difficult to transfect, such as nondividing primary cells. These advantages clearly compensate for the higher experimental error in comparison with the standard approach. Furthermore, we expect further refinements of this method (e.g., to identify FPs with optimized folding characteristics).

The FCS-based determination of concentrations of signaling proteins in both Jurkat cells and naïve human $CD4^+$ T cells provides new insights into the homeostasis of cellular signaling proteins. With membrane density and concentration correlating with surface area and volume, an increase in cell size may strongly affect the stoichiometry

of signaling proteins. Very clearly, with only one pair of cells having been investigated at this point, it is too early to draw conclusions about the general validity of this correlation. Therefore, it will be highly interesting to extend these analyses of protein concentrations to other cell types, especially pairs of cells of the same origin or cells at different stages of the cell cycle. Moreover, further research should address the impact of these differences in stoichiometry on the function of the signaling network.

SUPPORTING MATERIAL

Eleven sections, seven figures, three tables, and references are available at http://www.biophysj.org/biophysj/supplemental/S0006-3495(11)01203-3.

The authors thank Enrico Schleiff and Bé Wieringa for helpful discussions.

This work was supported by the Volkswagen Foundation (Nachwuchsgruppen an Universitäten, I 77/472).

REFERENCES

1. Bader, S., S. Kühner, and A. C. Gavin. 2008. Interaction networks for systems biology. *FEBS Lett.* 582:1220–1224.
2. Lidke, D. S., and B. S. Wilson. 2009. Caught in the act: quantifying protein behaviour in living cells. *Trends Cell Biol.* 19:566–574.
3. Dennis-Sykes, C. A., W. J. Miller, and W. J. McAleer. 1985. A quantitative Western blot method for protein measurement. *J. Biol. Stand.* 13:309–314.
4. Schilling, M., T. Maiwald, …, U. Klingmüller. 2005. Quantitative data generation for systems biology: the impact of randomisation, calibrators and normalisers. *Syst. Biol. (Stevenage).* 152:193–200.
5. Ong, S. E., B. Blagoev, …, M. Mann. 2002. Stable isotope labeling by amino acids in cell culture, SILAC, as a simple and accurate approach to expression proteomics. *Mol. Cell. Proteomics.* 1:376–386.
6. Gerber, S. A., J. Rush, …, S. P. Gygi. 2003. Absolute quantification of proteins and phosphoproteins from cell lysates by tandem MS. *Proc. Natl. Acad. Sci. USA.* 100:6940–6945.
7. Stoevesandt, O., M. Elbs, …, R. Brock. 2005. Peptide microarrays for the detection of molecular interactions in cellular signal transduction. *Proteomics.* 5:2010–2017.
8. Weidemann, T., M. Wachsmuth, …, J. Langowski. 2003. Counting nucleosomes in living cells with a combination of fluorescence correlation spectroscopy and confocal imaging. *J. Mol. Biol.* 334:229–240.
9. Rigler, R., Ü. Mets, …, P. Kask. 1993. Fluorescence correlation spectroscopy with high count rate and low background: analysis of translational diffusion. *Eur. Biophys. J.* 22:169–175.
10. Haustein, E., and P. Schwille. 2003. Ultrasensitive investigations of biological systems by fluorescence correlation spectroscopy. *Methods.* 29:153–166.
11. Brock, R., G. Vàmosi, …, T. M. Jovin. 1999. Rapid characterization of green fluorescent protein fusion proteins on the molecular and cellular level by fluorescence correlation microscopy. *Proc. Natl. Acad. Sci. USA.* 96:10123–10128.
12. Horejsí, V., W. Zhang, and B. Schraven. 2004. Transmembrane adaptor proteins: organizers of immunoreceptor signalling. *Nat. Rev. Immunol.* 4:603–616.
13. Paz, P. E., S. Wang, …, A. Abo. 2001. Mapping the Zap-70 phosphorylation sites on LAT (linker for activation of T cells) required for recruitment and activation of signalling proteins in T cells. *Biochem. J.* 356:461–471.
14. Zhang, W., R. P. Trible, …, L. E. Samelson. 2000. Association of Grb2, Gads, and phospholipase C-gamma 1 with phosphorylated LAT tyrosine residues. Effect of LAT tyrosine mutations on T cell antigen receptor-mediated signaling. *J. Biol. Chem.* 275:23355–23361.
15. Kosugi, A., J. Sakakura, …, T. Hamaoka. 2001. Involvement of SHP-1 tyrosine phosphatase in TCR-mediated signaling pathways in lipid rafts. *Immunity.* 14:669–680.
16. Jones, R. B., A. Gordus, …, G. MacBeath. 2006. A quantitative protein interaction network for the ErbB receptors using protein microarrays. *Nature.* 439:168–174.
17. Machida, K., C. M. Thompson, …, B. J. Mayer. 2007. High-throughput phosphotyrosine profiling using SH2 domains. *Mol. Cell.* 26:899–915.
18. Haupts, U., S. Maiti, …, W. W. Webb. 1998. Dynamics of fluorescence fluctuations in green fluorescent protein observed by fluorescence correlation spectroscopy. *Proc. Natl. Acad. Sci. USA.* 95:13573–13578.
19. Hendrix, J., C. Flors, …, Y. Engelborghs. 2008. Dark states in monomeric red fluorescent proteins studied by fluorescence correlation and single molecule spectroscopy. *Biophys. J.* 94:4103–4113.
20. Koppel, D. E. 1974. Statistical accuracy in fluorescence correlation spectroscopy. *Phys. Rev. A.* 10:1938–1945.
21. Shaner, N. C., R. E. Campbell, …, R. Y. Tsien. 2004. Improved monomeric red, orange and yellow fluorescent proteins derived from Discosoma sp. red fluorescent protein. *Nat. Biotechnol.* 22:1567–1572.
22. Bacia, K., S. A. Kim, and P. Schwille. 2006. Fluorescence cross-correlation spectroscopy in living cells. *Nat. Methods.* 3:83–89.
23. Stoevesandt, O., K. Köhler, …, R. Brock. 2005. One-step analysis of protein complexes in microliters of cell lysate. *Nat. Methods.* 2:833–835.
24. Patterson, G. H., S. M. Knobel, …, D. W. Piston. 1997. Use of the green fluorescent protein and its mutants in quantitative fluorescence microscopy. *Biophys. J.* 73:2782–2790.
25. Sugiyama, Y., I. Kawabata, …, S. Okabe. 2005. Determination of absolute protein numbers in single synapses by a GFP-based calibration technique. *Nat. Methods.* 2:677–684.
26. Dickson, R. M., A. B. Cubitt, …, W. E. Moerner. 1997. On/off blinking and switching behaviour of single molecules of green fluorescent protein. *Nature.* 388:355–358.
27. Sacchetti, A., V. Cappetti, …, S. Alberti. 2001. Green fluorescent protein variants fold differentially in prokaryotic and eukaryotic cells. *J. Cell. Biochem. Suppl.* 36 (*Suppl 36*):117–128.
28. Chang, H. C., C. M. Kaiser, …, J. M. Barral. 2005. De novo folding of GFP fusion proteins: high efficiency in eukaryotes but not in bacteria. *J. Mol. Biol.* 353:397–409.
29. Kremers, G. J., J. Goedhart, …, T. W. Gadella, Jr. 2007. Improved green and blue fluorescent proteins for expression in bacteria and mammalian cells. *Biochemistry.* 46:3775–3783.
30. Hamer, G., O. Matilainen, and C. I. Holmberg. 2010. A photoconvertible reporter of the ubiquitin-proteasome system in vivo. *Nat. Methods.* 7:473–478.
31. Yen, H. C., Q. Xu, …, S. J. Elledge. 2008. Global protein stability profiling in mammalian cells. *Science.* 322:918–923.
32. Rüttinger, S., V. Buschmann, …, F. Koberling. 2008. Comparison and accuracy of methods to determine the confocal volume for quantitative fluorescence correlation spectroscopy. *J. Microsc.* 232:343–352.
33. Dertinger, T., V. Pacheco, …, J. Enderlein. 2007. Two-focus fluorescence correlation spectroscopy: a new tool for accurate and absolute diffusion measurements. *ChemPhysChem.* 8:433–443.
34. Brock, R., M. A. Hink, and T. M. Jovin. 1998. Fluorescence correlation microscopy of cells in the presence of autofluorescence. *Biophys. J.* 75:2547–2557.
35. Bonello, G., N. Blanchard, …, Y. Collette. 2004. Dynamic recruitment of the adaptor protein LAT: LAT exists in two distinct intracellular pools and controls its own recruitment. *J. Cell Sci.* 117:1009–1016.
36. Nag, A., M. I. Monine, …, B. Goldstein. 2009. Aggregation of membrane proteins by cytosolic cross-linkers: theory and simulation of the LAT-Grb2-SOS1 system. *Biophys. J.* 96:2604–2623.

37. Hanke, S., H. Besir, …, M. Mann. 2008. Absolute SILAC for accurate quantitation of proteins in complex mixtures down to the attomole level. *J. Proteome Res.* 7:1118–1130.

38. Zheng, Y., V. Balakrishnan, …, A. Rundell. 2005. Modeling and analysis of early events in T-lymphocyte antigen-activated intracellular-signaling pathways. *J. Comput. Appl. Math.* 184:320–341.

39. Altan-Bonnet, G., and R. N. Germain. 2005. Modeling T cell antigen discrimination based on feedback control of digital ERK responses. *PLoS Biol.* 3:e356.

40. Wylie, D. C., J. Das, and A. K. Chakraborty. 2007. Sensitivity of T cells to antigen and antagonism emerges from differential regulation of the same molecular signaling module. *Proc. Natl. Acad. Sci. USA.* 104:5533–5538.

41. Zhu, M., E. Janssen, and W. Zhang. 2003. Minimal requirement of tyrosine residues of linker for activation of T cells in TCR signaling and thymocyte development. *J. Immunol.* 170:325–333.

42. Houtman, J. C., H. Yamaguchi, …, L. E. Samelson. 2006. Oligomerization of signaling complexes by the multipoint binding of GRB2 to both LAT and SOS1. *Nat. Struct. Mol. Biol.* 13:798–805.